CHAPTER I-2
THE INCREASE OF POLLUTANTS (NITROGEN OXIDES AND OZONE) IN THE SUMMERTIME MIDWEST

HIRAM LEVY II[1], JAMES J. YIENGER[1], WALTER J. MOXIM[1],
PRASAD S. KASIBHATLA[2] and WILLIAM L. CHAMEIDES[2]
[1]*Geophysical Fluid Dynamics Laboratory/NOAA, Princeton, New Jersey 08542;*
[2]*Earth and Atmospheric Sciences, Georgia Institute of Technology, Atlanta, Georgia 30332*

Abstract

We use the Geophysical Fluid Dynamics Laboratory (GFDL) Global Chemical Transport Model, with the six known sources for tropospheric NO_x and off-line calculations of daytime gas-phase nitrogen photochemistry and night-time heterogeneous chemistry, to simulate the summer time concentrations of reactive nitrogen compounds for pre-industrial, current and future emission scenarios. The simulated levels are less than 0.5 ppbv throughout the Midwest during the pre-industrial period. For present conditions, the simulated NO_x levels range from [1.5 - 2 ppbv] in the west to [5-10 ppbv] in the east and are in reasonable agreement with summertime measurements in Bondville, Illinois. We predict that NO_x levels will increase another 30% by 2020.

Using a simple relationship that relates NO_y and NO_x concentrations to the net chemical production of ozone at rural sites (Trainer *et al.* 1993), we estimate, conservatively, that the ozone, which was at relatively harmless levels in the pre-industrial period, is now at the crop-damage threshold of 50-70 ppbv in parts of Illinois, Indiana and Ohio. Furthermore, we estimate that this threshold will be reached throughout most of the Midwest east of the Mississippi River and even exceeded in parts of Illinois, Indiana, and Ohio by the year 2020, unless the continued increase in midwestern nitrogen fertilizer application and fossil fuel combustion ceases.

Introduction

The oxides of nitrogen, specifically $NO+NO_2$ (NO_x), are directly linked to the oxidizing efficiency of the troposphere by their ability to regulate the concentration of ozone (O_3) and hydroxyl radicals (OH) (Levy, 1971; Chameides and Walker, 1973; Crutzen, 1974, 1979). The photooxidation of CO, CH_4 and other hydrocarbons in the presence of elevated NO_x levels leads to the chemical production of ozone, elevated levels of which can both damage crops and cause human respiratory distress (*e.g.*, NAS Ozone Report). Noting that three regions of the northern mid-latitudes, labeled Continental-Scale Metro-Agro-Plexes (CSMAP's), dominate global industrial and agricultural activity, Chameides *et al.* (1994) recently proposed that current levels of NO_x emissions may have already elevated ozone levels enough to begin to reduce yields over 10%-35% of the world's grain producing regions. They predict that the level of exposure to yield-reducing ozone pollution may triple by 2025. For this study, we will focus on part of the North American CSMAP, the midwestern United States, and simulate the evolution of atmospheric NO_x levels in that region from pre-industrial times through the present and into the future (2020). We will determine the relative contributions from fertilizer application and fossil fuel combustion and, using the algorithm of Trainer *et al.*

Preparing for Global Change: A Midwestern Perspective, pp. 11–19
edited by G.R. Carmichael, G.E. Folk and J.L. Schnoor

(1993) [see discussion in Chameides *et al.*, 1994], estimate the potential elevation of ozone and its impact on crops.

NO_x emissions

Before there was a significant human presence on earth, NO_x sources in the midlatitudes were dominated by soil-biogenic emissions with lesser contributions from natural wildfires, lightning and stratospheric injection. Presently, there are six recognized sources: fossil fuel combustion, soil-biogenic emission, biomass burning, lightning discharge, upper troposphere aircraft emission, and stratospheric injection. The combustion of fossil fuel and soil-biogenic emissions are the dominant sources of NO_x in the modern CSMAP's of the northern midlatitudes. The fossil fuel source, which is both strong and localized, dominates in industrialized areas (Logan, 1983; Chameides *et al.*, 1994), while soil-biogenic emissions account for a large fraction of the total NO_x source in more rural areas and may even dominate in regions of intensive agriculture (Yienger and Levy, 1995). Both of these sources are expected to increase significantly by 2020-2025 (Galloway *et al.*, 1994; Chameides *et al.*, 1994; Yienger and Levy, 1995).

The natural NO_x source for the pre-industrial and pre-intensive agriculture simulation is composed of 3.6tgN/yr from unfertilized soil-biogenic emissions (Yienger and levy, 1995), 3tgN/yr from lightning (Levy and Moxim, 1994), 0.9tgN/yr from natural wildfires (Galloway *et al.*, 1994) and 0.6tgN/yr from the stratosphere. For the present case, we use 21.3tgN/yr from fossil fuel combustion (Levy and Moxim, 1989), 8.5tgN/yr from biomass burning (Levy *et al.*, 1991), 5.5tgN/yr from soil-biogenic emissions (Yienger and Levy, 1995), the same 3 tgN/yr from lightning and 0.65tgN/yr from the stratosphere (Kasibhatla *et al.*, 1991), and 0.45tgN/yr from aircraft (Kasibhatla, 1993). For the 2020 scenario, global emissions from fossil fuel combustion increase to 45.6tgN/yr (Galloway *et al.*, 1994) and soil-biogenic emissions, due to much higher levels of fertilization, increase to 6.9tgN/yr (Yienger and Levy, 1995). While the increase in fossil fuel dominates on a global scale, the increases in both anthropogenic sources are comparable in the midwestern United States.

Global chemical transport model

We explicitly separate reactive nitrogen (NO_y) into three classes of transported species; nitrogen oxides (NO_x = NO + NO_2), nitric acid (HNO_3), and PAN, which act as surrogates for insoluble inorganic, soluble inorganic, and insoluble reservoir organic species, respectively. The conservation equations for their mixing ratios are integrated globally, using a medium resolution 3-D global chemical transport model (GCTM), until all tropospheric distributions are equilibrated [for details see Mahlman and Moxim (1978), Appendix A in Levy *et al.* (1982), Section 2.1 in Levy and Moxim (1989). and Section 2 in Kasibhatla *et al.* (1993)]. The GCTM is driven by 6-hour time-averaged winds and a consistent total-precipitation field generated for 1 year only by the par-

ent general circulation model (GCM) that was integrated without diurnal insulation [see Section 2 of Mahlman and Moxim (1978) for a summary, and Manabe *et al.* (1974) and Manabe and Holloway (1975) for details]. The GCTM can not realistically simulate atmospheric fluctuations, with periods shorter than six hours nor can it examine diurnal or interannual variability. Both the parent GCM and the GCTM have the same resolution, a horizontal grid size of ~265 km, and 11 vertical levels at standard pressures of 990, 940, 835, 685, 500, 315, 190, 110, 65, 38, and 10 mb.

Dry deposition of NO_x and PAN over land, and of HNO_3 over land, oceans, ice, and snow is calculated on the assumption of a balance between surface deposition and the turbulent flux in the bottom half of the lowest model level [see Equation 2.2 in Kasibhatla *et al.*, 1993]. The individual deposition velocities are described in detail in section 3 in Kasibhatla *et al.* (1993). The wet removal scheme distinguishes between stable or shallow convective and deep convective precipitation. The fraction of HNO_3 removed from the grid is a function of the local precipitation rate, and the west removal tendency is also proportional to the local tracer mixing ratio [see Section 2 in Kasibhatla *et al.* (1991) for details].

Gas phase chemical interconversion rates among NO_x, HNO_3, and PAN are calculated off-line for specified 2-D NO_x, CO, CH_4, non-methane hydrocarbons (NMHC), O_3 and H_2O fields using a standard chemical scheme (*e.g.*, Chameides and Tan, 1981) and are carried in the GCTM as temporally-varying, two-dimensional zonal fields. The thermal decomposition rate of PAN is calculated on-line as a function of the local model temperature. All specified fields, with the exception of NMHC, are described in Kasibhatla *et al.* (1991). The NMHC fields (Kanakidou *et al.*, 1991) are discussed in Section 2 of Kasibhatla *et al.*, 1993.

The three-dimensional rates for the nighttime heterogeneous conversion of NO_x to HNO_3 on sulfate aerosol, are also determined off-line by solving the 3 time-dependent equations for NO_2, NO_3, and N_2O_5. Monthly averaged 10°x10° fields of sulfate aerosol surface area (Dentener, 1993), local model temperatures and the two-dimensional ozone fields discussed above are used in the calculation.

NO_x fields

While much lower than present levels, the NO_x mixing ratios in the pre-industrial Midwest, driven by natural biogenic emissions from the tall- and short-grass prairies, were sufficient to support a small photochemical net-production of ozone (1-4 ppbv). Unlike the anthropogenic cases to be discussed next, the NO_x levels, which range from 0.1-1.0 ppbv, increase from east to west as vegetation switches from forest to grassland. Because of the significant temperature dependence for biogenic emissions from grasslands [See Fig. 4b in Yienger and Levy, 1995], the NO_x maximum occurs at the southern end of these grasslands. With the parent climate model's tendency towards excessive summer heat and dryness in mid-continent, the actual NO_x levels are probably

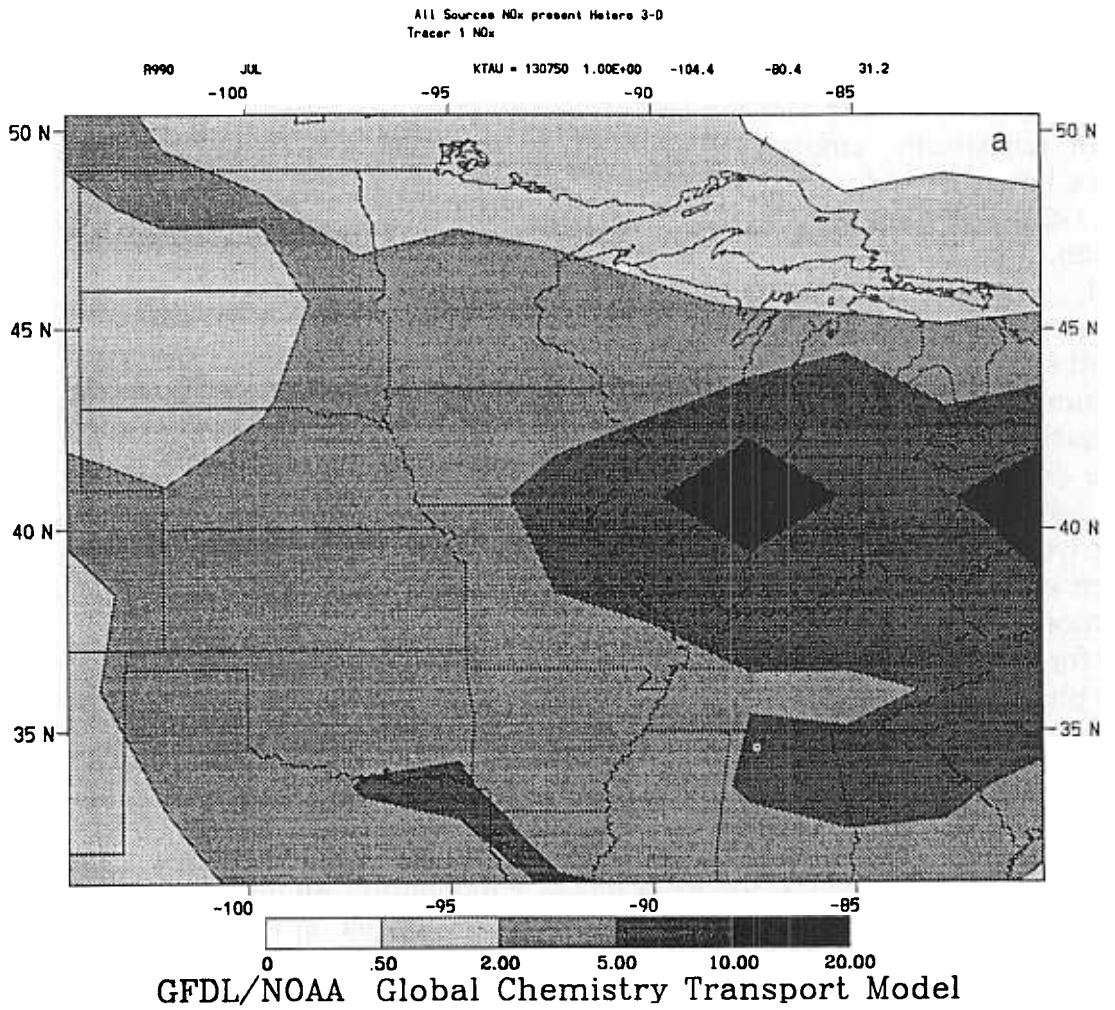

Fig. I-2.1a. Simulated July monthly-average surface NO_x mixing ratios [ppbv] for present conditions.

an upper-limit. However, the spatial pattern should be correct, and the levels would still be high enough for a small net chemical production of ozone.

The simulated monthly averaged July surface NO_x mixing ratios for the present and future are given in Fig.s I-2.1a-1b. With the current levels of anthropogenic emissions, NO_x levels have increased greatly throughout the midwest (1.5-10.0 ppbv), though now the mixing ratio maximum is in the east as the emissions from combustion begin to dominate. In the western portion and particularly in the northwest, soil biogenic emissions account for ~50% of the total NO_x (1-3 ppbv), while, in the more industrial eastern section, they only account for 10-20% of the total (5-10 ppbv). In Illinois, the simulated levels of NO_x range from 5-9 ppbv while summertime measurements from central Illinois (Bondville) give a daytime median of 2.5 ppbv and a night time median of 9 ppbv (Parrish *et al.*, 1993). Because of the 270 km grid size and horizontal sub-grid scale diffusion, the simulation for central Illinois is significantly contaminated by the very high emission from the greater Chicago area. With its lack of a diurnal cycle in the boundary layer mixing, a comparison of the

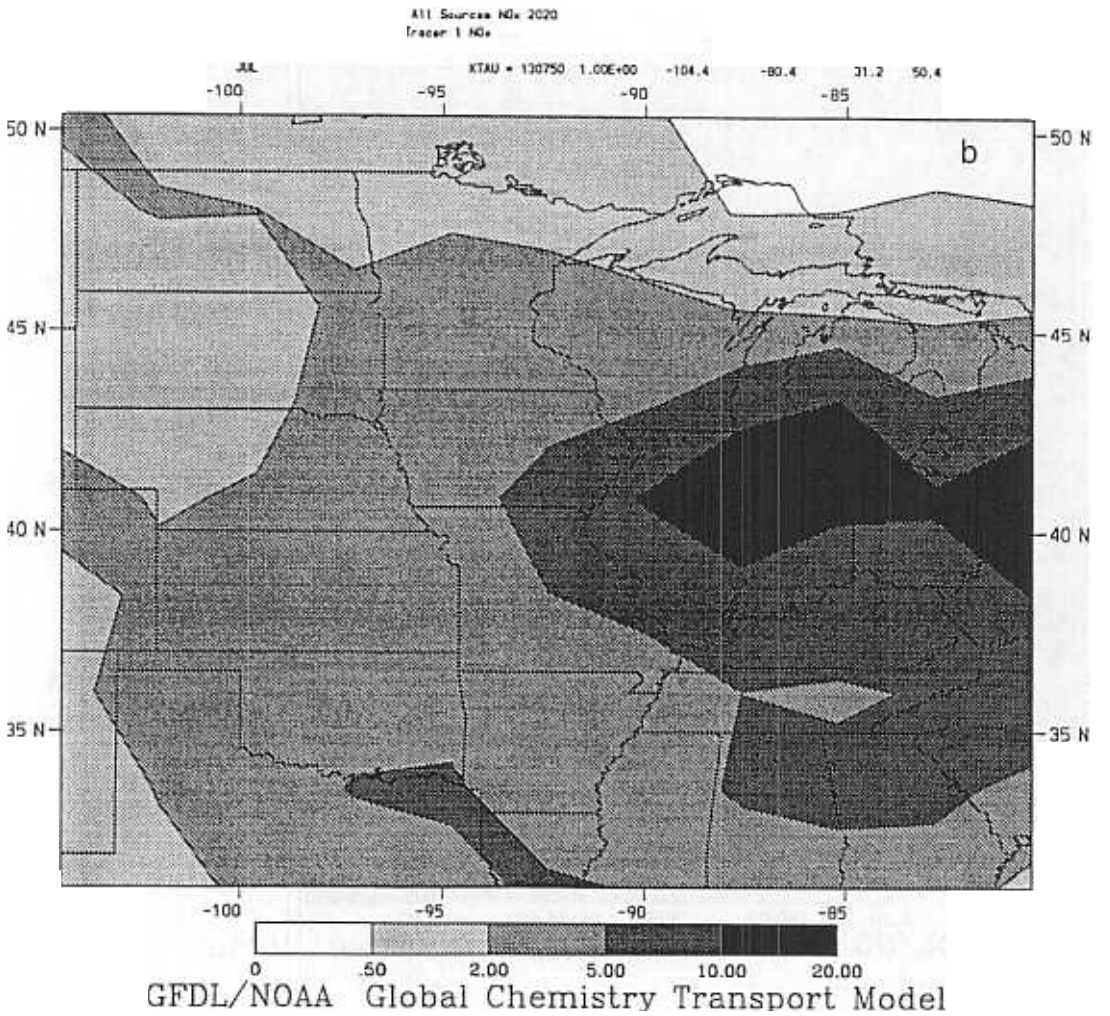

Fig. I-2.1b. Simulated July monthly-average surface NO_x mixingm ratios [ppbv] for estimated future emissions [2020-2025].

model with the daily average observations (~6 ppbv) may be appropriate. While the model's simulation may be high, it is clear that both the simulated and the observed levels of NO_x are more than sufficient for the net photochemical production of ozone (Trainer *et al.*, 1993).

The simulation for the future (2020) scenario finds an approximate 30% increase in NO_x levels throughout the midwest. This increase is driven by increased fertilizer use in the western portion and increased fossil fuel use in the eastern half. The pattern of the NO_x distribution is not significantly changed. The key issue is the impact of elevated NO_x levels on ozone pollution in the midwest. This is discussed in the next section.

Empirical ozone fields

While the ultimate answer to the impact of past, present, and future NO_x levels on midwestern ozone pollution awaits a chemical transport study with a

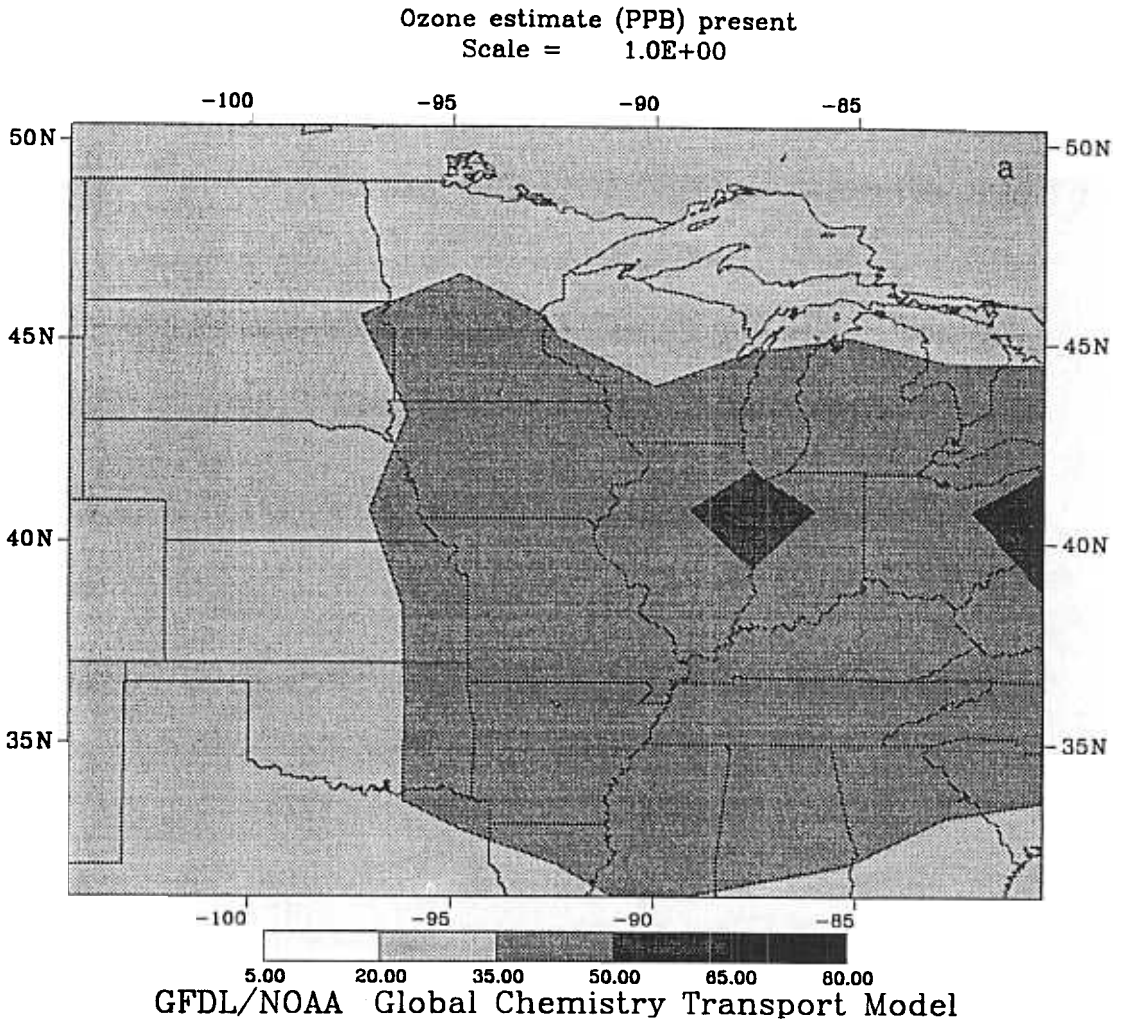

Fig. I-2.2a. Simulated July monthly-average surface Ozone mixing ratios [ppbv] for present NO_x emission levels.

detailed in situ chemical model, it is possible to estimate the impact with the aid of an empirical relationship between NO_x, NO_y, and O_3 that is discussed in Trainer *et al.* (1993).

$$\text{polluted ozone} = \text{background ozone} + k\,(NO_y - NO_x) \qquad (1)$$

Trainer et al (1993) propose a value of k = 8.5, based on their study of 6 rural sites in the eastern U.S. stretching from Bondville, Illinois to Whiteface Mt., New York. However, they note that the actual value of k tends to be positively correlated with the concentration of reactive hydrocarbon and Chameides *et al.* (1994) suggest a range of 5 to 13 for k. Assuming that much of the Midwest is or was grassland or cultivated land, rather than forest (*i.e.*, that reactive hydrocarbon concentrations are lower than those in the East), and suspecting that the simulated NO_x and NO_y levels are somewhat high, as discussed previously, we have chosen to make a conservative estimate of the possible levels of ozone pollution and use k = 5. For the background O_3, we use a simulation that assumed only a stratospheric source with both chemical

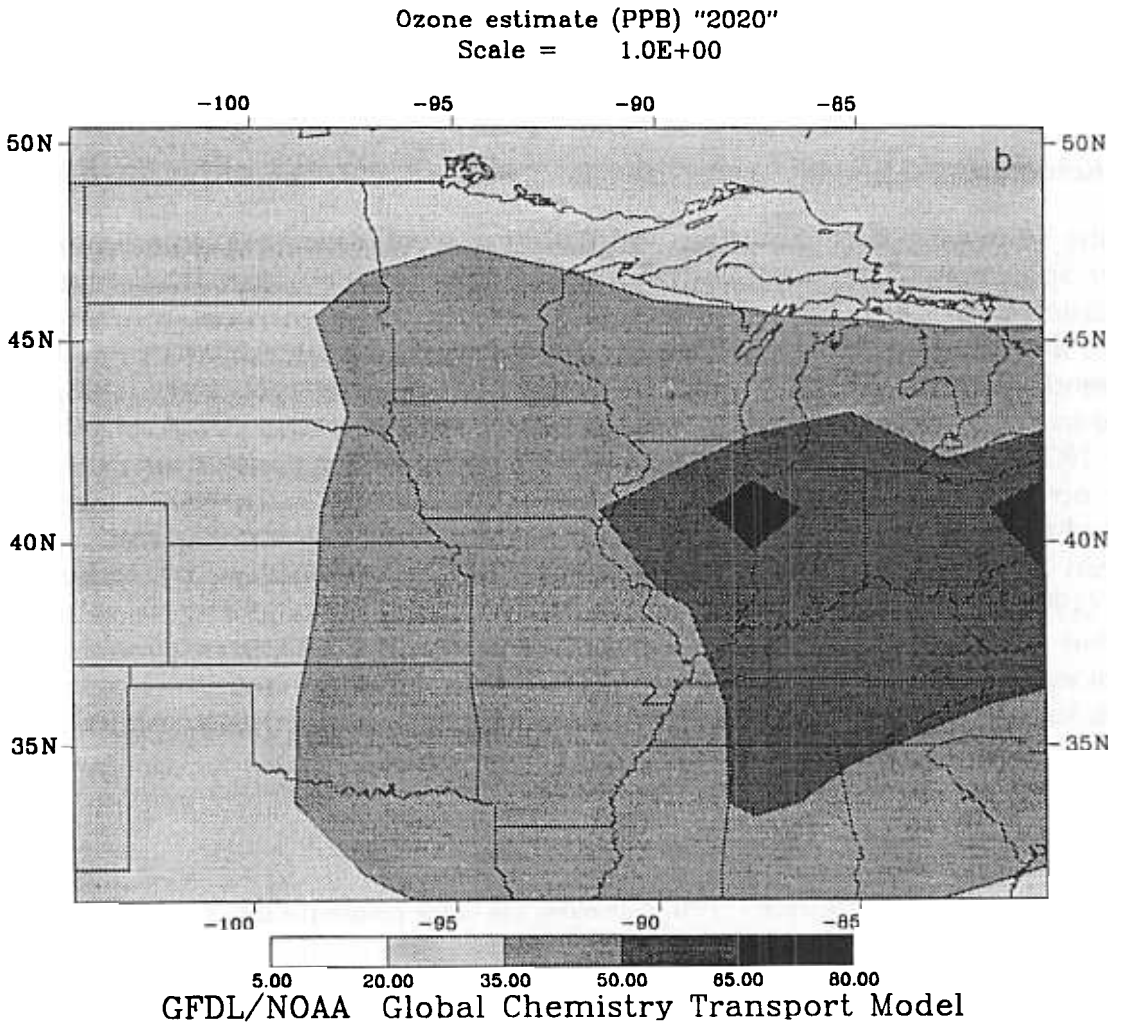

Fig. I-2.2b. Simulated July monthly-average surface Ozone mixing ratios [ppbv] for future ("2020") NO_x emission levels.

destruction in the atmospheric boundary layer and surface deposition as the loss paths (Levy *et al.*, 1985; unpublished results).

While we estimate a small net chemical production of ozone, the resulting average July values for the pre-industrial Midwest are generally below 30 ppbv and would have been of no danger to the environment. However, the simulated present and future O_3 levels (see Fig.s I-2.2a and I-2.2b) are a different story. As discussed in Chameides *et al.* (1994) and references contained therein, ozone levels in the range of 50-70 ppbv begin to lower crop yield. While an accurate assessment of the impact requires the calculation of an integrated ozone dosage rather than just the monthly average value, these estimates should raise some warnings. Even using the conservative value, k - 5, we find that average July ozone levels, while below the 50 ppbv in much of the Midwest, have already reached the 50-70 ppbv threshold in part of Illinois, Indiana, and Ohio. In the 2020 simulation, July average ozone levels exceed 70 ppbv in parts of Illinois, Indiana, and Ohio and they reach the threshold

level all the way to the Mississippi River. If the value k = 8.5 is used, as recommended by Trainer *et al.* (1993), almost all of the Midwest is predicted to fall within the 50-70 ppbv ozone threshold for crop damage by 2020.

Conclusions

In the Midwest before the advent of fossil fuel combustion and intensive fertilizer application, NO_x concentrations were controlled by natural soil biogenic emissions and O_3, which was controlled by the natural process of injection from the stratosphere, was of no danger to the environment. With the advent of modern industry, intensive agriculture and automobiles and trucks, this picture has changed significantly and is predicted to continue to do so. Midwestern NO_x levels, while generally lower than those in the major urban centers, are now capable of significant net chemical production of pollution ozone. Based on our simulations of NO_x and background O_3 and the relationship between NO_x, NO_y and the chemical production of O_3 proposed by Trainer *et al.* (1993), we estimate that parts of Illinois, Indiana and Ohio are already within the O_3 threshold for crop damage and that, by 2020, most of the Midwest east of the Mississippi River will be in that position, unless the two dominant sources of pollution NO_x, fossil fuel combustion and fertilizer application, are not permitted to grow.

References

NAS (National Academy of Sciences). 1991. Rethinking the ozone problem in urban and regional air pollution, Washington D.C., *National Academy Press.*

Chameides, W.L., P.S. Kasibhatla, J.J. Yienger, H. Levy II, and W.J. Moxim. 1994. The growth of continental-scale metro-agro-plexes, regional ozone pollution, and world food production. *Science*, in press.

Chameides, W.L. and A. Tans. 1981. The two-dimensional diagnostic model for tropospheric OH: An uncertainty analysis. *J. Geophys. Res.*, 86, 5209-5223.

Chameides, W.L., and J.C.G. Walker. 1973. A photochemical theory of tropospheric ozone. *J. Geophys. Res.*, 78, 8751-8760.

Crutzen, P.J. 1974. Photochemical reaction initiated by and influencing ozone in unpolluted tropospheric air. *Tellus*, 26, 45-55.

Crutzen, P.J. 1979. The role of NO and NO_2 in the chemistry of troposphere and stratosphere. *Annu. Rev. Earth Planet Sci.*, 7, 443-472.

Dentener, F.J. and P.J. Crutzen. 1993. Reaction of N_2O_5 on tropospheric aerosols: Impact on the global distributions of NO_x, O_3, OH. *J. Geophys. Res.*, 98, 7149-7163.

Galloway, J.N., H. Levy II, and P.S. Kasibhatla. 1994. Year 2020: Consequences of population growth and development on deposition of oxidized nitrogen. *Ambio*, 23, 120-123.

Kanakidou, M., H.B. Singh, K.M. Valentin, and P.J. Crutzen, 1991. A two-dimensional study of ethane and propane oxidation in the tropopshere. *J. Geophys. Res.*, 96, 15395-15425.

Kasibhatla, P.S. 1993. NO_y from sub-sonic aircraft emissions: A global three-dimensional model study. *Geophys. Res. Lett.*, 20, 1707-1710.

Kasibhatla, P.S., H. Levy II, W.J. Moxim, and W.L. Chameides, 1991. The relative impact of stratospheric photochemical production on tropospheric NO_y levels: A model study. *J. Geophys. Res.*, 96, 18631-18646.

Kasibhatla, P.S., H. Levy II, and W.J. Moxim, 1993. Global NO_x, HNO_3, PAN and NO_y distributions from fossil-fuel combustion emissions: A model study. *J. Geophys. Res.*, 98, 7165-7180.

Levy II, H. 1971. Normal atmosphere: Large radical and formaldehyde concentrations predicted. *Science*, 173, 141-143.

Levy II, H., J.D. Mahlman, and W.J. Moxim, 1982. Tropospheric N_2O variability. *J. Geophys. Res.*, 87, 3061-3080.

Levy II, H., J.D. Mahlman, W.J. Moxim, and S.C. Liu, 1985. Tropospheric ozone: The role of transport. *J. Geophys.Res.*, 90, 3753-3772.

Levy II, H., and W.J. Moxim, 1989. Simulated global distribution and deposition of reactive nitrogen emitted by fossil fuel combustion. *Tellus*, 41, 256-271.

Levy II, H., W.J. Moxim, P.S. Kasibhatla, and J.A. Logan, 1991. The global impact of biomass burning on tropospheric reactive nitrogen. In: w*Global Biomass Burning: 'Atmospheric, Climatic, and Biospheric Implications*, J.S. Levine, Editor, p. 363-369, MIT Press, Cambridge, MA.

Levy II, H., and W.J. Moxim, 1994. Global lightning sources of NO_x. (in preparation)

Mahlman, J.D. and W.J. Moxim, 1978. Tracer simulation using a global general circulation model: Results from a midlatitude instantaneous source experiment. *J. Atmos. Sci.*, 35, 1340-1374.

Logan, J.A., 1983. Nitrogen oxides in the troposphere: Global and regional budgets. *J. Geophys. Res.*, 88, 10785-10807.

Manabe, S., D.G. Hahn, and J.L. Holloway, R. 1974. The seasonal variation of the tropical circulation as simulated by a global model of the atmosphere. *J. Atmos. Sci*, 31, 43-83.

Manabe, S., and J.L. Holloway, Jr., 1975. The seasonal variation of the hydrologic cycle as simulated by a global model of the atmosphere. *J. Geophys. Res.*, 80, 1617-1649.

Parrish, D.D., *et al.*, 1993. The total reactive oxidized nitrogen levels and the partitioning between the individual species at 6 rural sites in eastern North America. *J. Geophys. Res.*, 98, 2927-2939.

Trainer, M., *et al.*, 1993. Correlation of ozone with NO_y in photochemically aged air. *J. Geophys. Res.*, 98, 2917-2925.

Yienger, J.J. and H. Levy II, 1995. Global inventory of soil-biogenic NO_x emissions, *J. Geophys. Res.*, in press.